The Influence of Turbulent Mixing on Deflagration to Detonation Transition

Brian Maxwell , Matei Radulescu
Department of Mechanical Engineering, University of Ottawa
161 Louis Pasteur, Ottawa, K1N 6N5, Canada

Andrzej Pekalski
Shell Global Solutions, UK

1 Introduction

In the current study, the influence of *turbulent mixing* on Deflagration to Detonation Transition (DDT) is investigated, using a state-of-the-art Large Eddy Simulation (LES) strategy, for conditions which correspond to recent experiments [1–3]. This investigation follows the procedure of Radulescu and Maxwell [4] by considering the re-ignition of fully quenched detonations, following the detonation interaction with a porous medium, as shown in Figure 1. This type of DDT has also been examined experimentally for detonation interactions with perforated plates [5], or a series of obstacles, or blockages [6, 7]. Currently, the quenching process of detonations is well understood. As a detonation wave diffracts around an object, the sudden change in area causes volumetric expansion of the gas behind the leading shock wave. Eventually, the detonation can become quenched when local cooling due to this expansion overcomes local heating due to chemical reactions [8–10]. The result is a de-coupling between the leading shock wave and reaction zone, as observed experimentally [11, 12]. The re-initiation process, however, is not so clear. To date, it has been found that re-initiation of the attenuated detonation wave occurs through amplification of the incident shock strength resulting from shock reflections or triple point collisions [4, 13]. In some cases, several shock reflections are required to accelerate the leading shock wave sufficiently in order to re-initiate the detonation. At each shock reflection, or triple point collision, the incident shock is accelerated due to increased reaction rates in the un-burned gases behind the incident shock. In similar experiments, which examined *quasi-detonation* propagation in porous media [14–16], it has been shown that a wave can be sustained below the steady Chapman-Jouguet (CJ) detonation velocity. Due to the velocity deficit, it is believed that *adiabatic compression* alone, from shock interactions, cannot provide the necessary ignition to sustain a detonation wave. Thus, it remains unclear whether adiabatic shock compression or turbulent mixing is the dominant mechanism that drives, or initiates, the detonation.

More recently, experiments at the University of Ottawa [2, 3], have correlated detonation re-initiation events to a stability criterion, the χ parameter [17], which is the product of the mixture activation energy and the ratio of chemical induction to reaction time. The transition length to initiate a self-sustained detonation was found to correlate very well with the mixtures sensitivity to temperature fluctuations. Thus, it was found that DDT events were more likely to occur as the mixture irregularity increased. Furthermore, it was also found that a necessary condition for DDT was the acceleration of the flame to the critical CJ *deflagration*

Correspondence to: bmaxwell@uottawa.ca

velocity [3]. Since irregular mixtures contain highly turbulent flow fields, it is therefore likely that turbulent mixing is a dominant mechanism that influences the DDT process. To what extent, however, is the topic of investigation below.

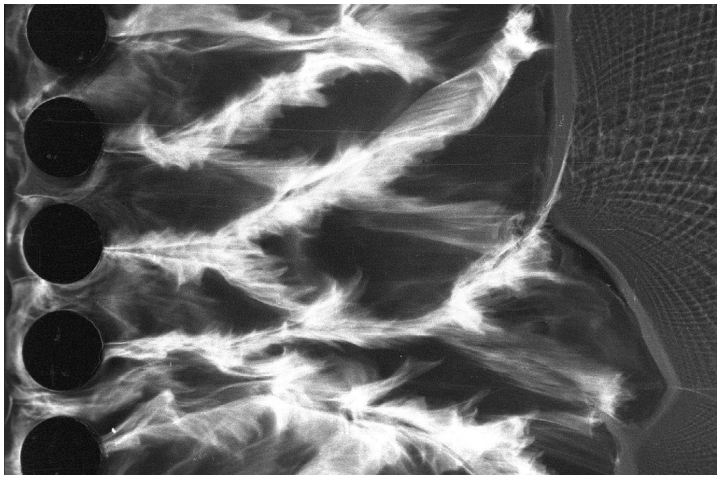

Figure 1: Open shutter photograph showing DDT of $C_2H_2 + O_2$ at $\hat{p}_o = 5$kPa, following detonation interaction with a porous medium [4].

In the current work, detonation attenuation by a porous medium, as depicted in Figure 1, and the subsequent re-initiation is modelled, numerically, using the Compressible LEM-LES (CLEM-LES) approach [18]. This approach is a grid-within-a-grid approach, based on the Linear Eddy Model for Large Eddy Simulation (LEM-LES) [19]. The CLEM-LES was recently validated to experiments and applied to investigate the role of *turbulent mixing* on unobstructed, irregular detonation propagation in a narrow channel filled with premixed methane-oxygen at low pressures [18, 20]. In this recent investigation, it was found that altering the turbulent mixing rates had a significant impact on the detonation hydrodynamic structure, cell size, and formation of un-burned pockets in the wake. In the current study, the same approach was adopted: To validate DDT events observed in numerical simulations with experimental observations, and to determine how such events are influenced by changes in the turbulent fluctuations present.

2 Modelling Approach: Filtered LES Equations and Subgrid Models

For flows which are highly transient, turbulent, compressible, and involve rapid combustion chemistry, the gas dynamic evolution is governed by the compressible N-S equations. In order to address the difficulty of resolving the full spectrum of length scales resulting from the presence of large flow velocities with high Mach numbers (M_a) and Reynolds numbers (R_e), the unresolved scales of the governing equations are filtered and modelled through the LES approach. In this respect, rapid transients and fluid motions are captured on the large scales, while the small scale contributions are modelled through source terms. The LES-filtered conservation equations for mass, momentum, and energy of a calorically perfect fluid system are given below in Equations (1) through (3), respectively. The set of equations is further supplemented by a one-equation Localized Kinetic energy Model (LKM) to describe the evolution of sub-grid velocity fluctuations in the form of sub-grid kinetic energy k^{sgs}, see Equation (4). Finally, the equations of state are given by (5). The equations are given in non-dimensional form where the various gas properties are normalized by the reference quiescent state. Favre-average filtering is achieved by letting $\tilde{f} = \overline{\rho f}/\bar{\rho}$, where f represents one of the many state variables. Here ρ, p, e, T, and $\boldsymbol{u}$ refer to density, pressure, specific sensible + kinetic energy, temperature, and velocity vector, respectively.

$$\frac{\partial \bar{\rho}}{\partial t} + \nabla \cdot (\bar{\rho}\tilde{\boldsymbol{u}}) = 0 \tag{1}$$

$$\frac{\partial \bar{\rho}\tilde{\boldsymbol{u}}}{\partial t} + \nabla \cdot (\bar{\rho}\tilde{\boldsymbol{u}}\tilde{\boldsymbol{u}}) + \nabla \bar{p} - \nabla \cdot \bar{\rho}(\nu + \nu_t)\left(\nabla \tilde{\boldsymbol{u}} + (\nabla \tilde{\boldsymbol{u}})^T - \frac{2}{3}(\nabla \cdot \tilde{\boldsymbol{u}})\hat{I}\right) = 0 \tag{2}$$

$$\frac{\partial \bar{\rho}\tilde{e}}{\partial t} + \nabla \cdot \left((\bar{\rho}\tilde{e} + \bar{p})\tilde{\boldsymbol{u}} - \tilde{\boldsymbol{u}} \cdot \bar{\tau} \right) - \left(\frac{\gamma}{\gamma - 1} \right) \nabla \cdot \left(\bar{\rho} (\frac{\nu}{P_r} + \frac{\nu_t}{P_{r,t}}) \nabla \tilde{T} \right) = -Q\bar{\dot{\omega}} \tag{3}$$

$$\frac{\partial \bar{\rho} k^{sgs}}{\partial t} + \nabla \cdot (\bar{\rho}\tilde{\boldsymbol{u}} k^{sgs}) - \nabla \cdot \left(\frac{\bar{\rho}\nu_t}{P_{r,t}} \nabla k^{sgs} \right) = \bar{\rho}\nu_t \left(\nabla \tilde{\boldsymbol{u}} + (\nabla \tilde{\boldsymbol{u}})^T - \frac{2}{3} (\nabla \cdot \tilde{\boldsymbol{u}}) \hat{I} \right) \cdot (\nabla \tilde{\boldsymbol{u}}) - \bar{\rho}\epsilon \tag{4}$$

$$\tilde{e} = \frac{\bar{p}/\bar{\rho}}{(\gamma - 1)} + \frac{1}{2}\tilde{\boldsymbol{u}}\tilde{\boldsymbol{u}} + \frac{1}{2} k^{sgs} \qquad \text{and} \qquad \bar{\rho}\tilde{T} = \bar{p} \tag{5}$$

Other usual properties to note are the heat release, Q, the ratio of specific heats, γ, and the kinematic viscosity, ν. The turbulent viscosity and dissipation are modeled according to

$$\nu_t = \frac{1}{\pi} \left(\frac{2}{3 C_\kappa} \right)^{3/2} \sqrt{k^{sgs}} \bar{\Delta} \tag{6}$$

and

$$\epsilon = \pi \left(\frac{2 k^{sgs}}{3 C_\kappa} \right)^{3/2} / \bar{\Delta} \tag{7}$$

respectively. Here, $\bar{\Delta}$ is the minimum grid spacing, and C_κ is the *Kolmogorov* number, a model parameter which requires calibration. Finally, the chemical reaction term, $\bar{\dot{\omega}}$, requires closure.

In order to close the chemical reaction term, $\bar{\dot{\omega}}$, the CLEM sub-grid modelling strategy is applied. Here, the micro-scale mixing and chemical reaction is handled entirely on the sub-grid, through a supplementary simulation of a 1D sample of the flow field within each LES cell. The system of equations that is solved on the sub-grid is the conservation of enthalpy, Equation (8), and the conservation of reactant mass, Equation (9). The source terms, $\dot{F}_T$ and $\dot{F}_Y$ account for the effect of turbulence on the sub-grid in the form of random "stirring" events [19] and $\dot{p}$ accounts for the energy changes associated with rapid changes in pressure, which is obtained entirely from the large-scale simulation, Equations (1) to (4). Next, m is a one-dimensional mass weighted coordinate whose transformation to Cartesian spatial coordinates is given by Equation (10). Finally, a one-step Arrhenius combustion model is assumed through Equation (11), which uses a single reactant species, with mass fraction Y. Full details of the procedure, including the pressure coupling and LEM stirring, are found elsewhere [18].

$$\rho \frac{DT}{Dt} - \left(\frac{\gamma - 1}{\gamma} \right) \dot{p} - \rho \frac{\partial}{\partial m} \left(\rho^2 \frac{\nu}{P_r} \frac{\partial T}{\partial m} \right) = - \left(\frac{\gamma - 1}{\gamma} \right) Q\dot{\omega} + \dot{F}_T \tag{8}$$

$$\rho \frac{DY}{Dt} - \rho \frac{\partial}{\partial m} \left(\rho^2 \frac{\nu}{L_e P_r} \frac{\partial Y}{\partial m} \right) = \dot{\omega} + \dot{F}_Y \tag{9}$$

$$m(x,t) = \int_{x_o}^{x} \rho(x,t) dx \tag{10}$$

$$\dot{\omega} = -\rho A Y e^{(-E_a/T)} \tag{11}$$

3 Numerical Domain

A two-dimensional domain is considered with initial conditions and model parameters consistent with physical experiments [1–3], where detonation waves are first attenuated using a bank of cylinders, as shown in Figure 2. Here, the steady Zeldovich, Von Neumann, and Doring (ZND) detonation wave solution is imposed 9 half-reaction lengths, $\Delta_{1/2}$, upstream from a bank of 5 cylinders, with a blockage ratio of 75%.

The test section measures $500\Delta_{1/2}$ by $40\Delta_{1/2}$, which is comparable to the physical experiments [1–3]. Symmetric boundary conditions are considered on the top and bottom walls, with inlet and outlet boundary conditions at the domain ends as shown. The inlet boundary is sufficiently far from the test section ($200\Delta_{1/2}$) such that the results are unaffected by its influence. The model parameters, Q and E_a, are tuned to reproduce the correct post-shock ignition delay times for premixed methane-oxygen, a moderately unstable mixture. Here, $Q = 52.5$ and $E_a = 46.0$. The resolution used is $\bar{\Delta} = \Delta_{1/2}/32$, with an additional 16 sub-grid elements within each LES cell, for an effective resolution of $\bar{\Delta}_{eff} = \Delta_{1/2}/512$. This resolution was previously shown to resolve the post-shock laminar flame speeds and detonation structure for this particular methane-oxygen mixture [18]. Finally, C_κ is varied in order to change the amount of turbulent velocity fluctuations generated by the wave dynamics, and to consequently research it's affects on DDT.

4 Results

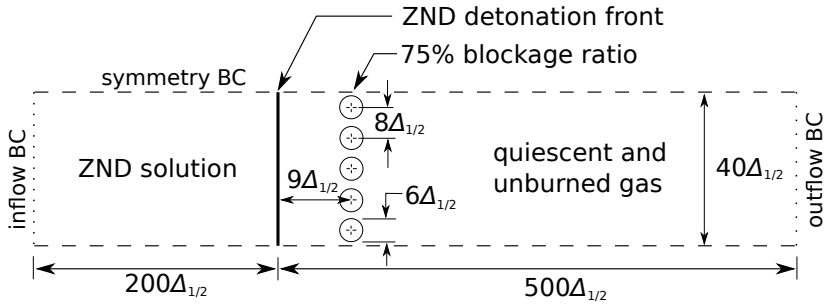

Figure 2: Numerical domain.

In this study, several simulations where conducted for C_κ values ranging from 2.0 to 3.0. The density evolution of a case where DDT occurs downstream from the obstacles, when $C_\kappa = 2.6$, is shown in Figure 3. Also shown is the corresponding numerical soot foil, which shows the regions of high vorticity, integrated over time. Just following the initial detonation interaction with the bank of cylinders, the detonation is effectively quenched. This is observed by the decoupling of the flame from the leading shock wave, which leads to a thickening of the reaction zone, as seen in frame (a) of Figure 3. Furthermore, turbulent motions give rise to the pattern observed in this frame. By frames (b) and (c), turbulent instabilities intensify, giving rise to a larger cellular structure. This is observed by the progressive increase of cell sizes in the corresponding numerical soot foil. This tendency of the deflagration cell structure to enter larger modes was also observed experimentally [1]. By frame (d), the deflagration cell structure spans the height of the domain. At this point detonation occurs through collision of the shock triple point with the upper wall, around $x \approx 170\Delta_{1/2}$, giving rise to close coupling between the reaction zone and leading shock, and a much smaller and more prominent cellular pattern on the numerical soot foil. In frame (e), detonation initiates at a separate location along the bottom wall, around $x \approx 180\Delta_{1/2}$. Finally, by frame (f), the entire wave front exists as a detonation.

The onset of detonation in this case was confirmed by measuring the velocity of the wave on the top wall, as a function of distance downstream from the obstacle centres, as shown in Figure 4. For $C_\kappa = 2.6$, prior to detonation, the observed wave speed is found to correspond to the CJ-deflagration speed, $D = 3.95$, as indicated in the figure. Eventually, detonation occurs and the wave travels at a much faster velocity; the CJ detonation velocity of $D = 6.43$. The results from the corresponding physical experiments [1, 2] are also shown in Figure 4. In Maley [1], the quenched wave is observed to travel near the CJ-deflagration speed, and shows signs of acceleration to the CJ-deflagration value when $x > 200\Delta_{1/2}$. In fact, detonation was observed at $x \approx 235\Delta_{1/2}$, near the end of the experimental test section. Unfortunately, velocity recordings beyond this point are not available. However, Ahmed's experiment [2] shows the same trend as the numerical simulation leading to DDT, where initially the wave velocity corresponds to the CJ-deflagration speed, and eventually accelerates to the CJ-detonation value by $x \approx 150\Delta_{1/2}$. Also shown in Figure 4 are the results

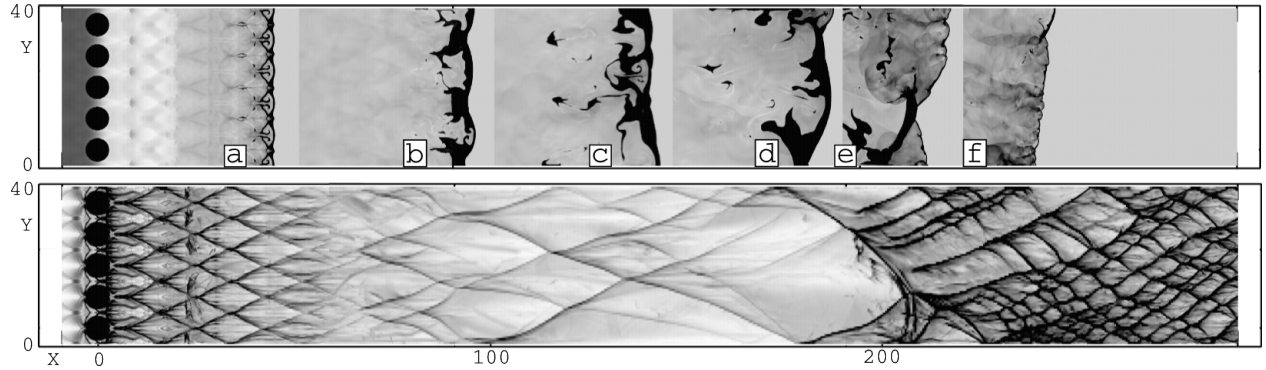

Figure 3: Density evolution (top) and corresponding numerical soot foil (bottom) obtained for $C_\kappa = 2.6$.

from simulations where $C_\kappa = 2.0$ and 3.0, with lower and higher turbulence intensities respectively. In these cases, the wave speed drops below the CJ-deflagration value, and detonation does not re-initiate for the duration of the simulation.

5 Discussion

In the current study, it is clear that sufficient turbulent mixing rates are required in order for DDT to occur. When $C_\kappa = 2.0$, the wave speed is unable to maintain a velocity above the CJ-deflagration value, and DDT does not occur. As C_κ is increased to 2.6, the turbulent mixing rates are also increased. This allows for increased reaction rates at surfaces of un-burned fuel in the wake of the wave front. As a result, the wave velocity is maintained above the CJ-deflagration speed. DDT then occurs in regions where triple point collisions occur. During these collision events, sufficient energy deposition due to shock compression coupled with intense turbulent burning allows for a localized detonation to form, which eventually consumes the entire wave front. In this case, combustion rates are locally enhanced by turbulence, which thus contribute to DDT as observed in shock-flame interaction experiments [21]. As C_κ is further increased to 3.0, however, DDT is once again mitigated. For sufficiently high turbulence intensity, it is believed that hot spots are transported away from the regions of high pressure and temperature, which thus prevent the local conditions necessary for DDT to occur. As a result, the wave speed remains below the CJ-deflagration threshold for the duration of the simulation. This form of DDT mitigation is believed to be related to flame extinction, which can occur given sufficient turbulence intensity [22]. Finally, it is noted that the required value of C_κ for DDT of methane-oxygen is much lower than previous simulations of the corresponding detonation propagation phase [20], where the optimal value was found to be $C_\kappa \geq 6.7$.

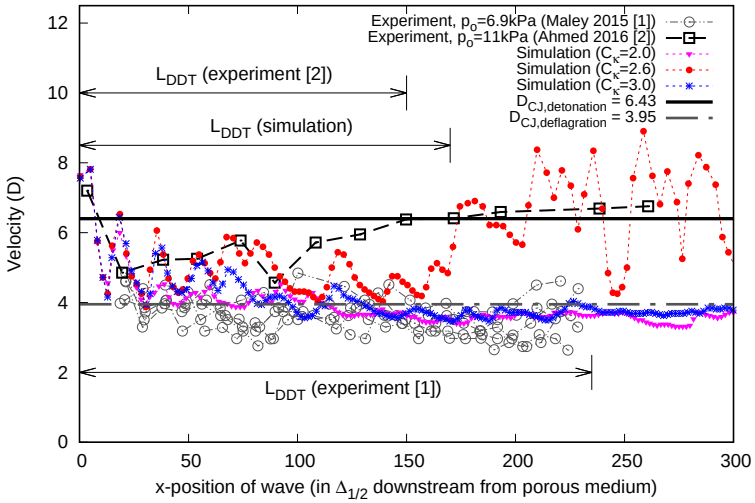

Figure 4: Wave velocity, as a function of distance, for a range of C_κ. Also shown are the correponding experimental results [1, 2], obtained for methane-oxygen at $\hat{p}_o = 6.9$kPa and $\hat{p}_o = 11.0$kPa, respectively.

6 Conclusion

In the current study, it was found, through numerical simulation, that turbulent mixing rates play a major role which contribute to, or mitigate, DDT events in methane-oxygen at low pressures. Furthermore, in order for detonation to occur, it was found that wave speeds must accelerate to, and sustain, the CJ-deflagration speed. This confirms earlier postulations, obtained from experiment [2,3], which require the CJ-deflagration speed as a precursor to detonation. It was found that a sufficient amount of turbulence intensity generation behind the wave front was required in order to maintain wave speeds above this CJ-deflagration threshold, thus allowing for the necessary conditions in order for DDT to occur. In addition to this, it was found that a further increase in turbulent mixing rates can also have a mitigation effect on DDT. Thus, detonation initiation events are very sensitive to changes in turbulence intensity. Therefore, there exists a an optimal range of C_κ in order to provide the necessary conditions, and combustion regime, for detonation to occur.

Funding for this project was provided by Shell and NSERC, through a Collaborative Research Grant.

References

[1] L. Maley, "On shock reflections in fast flames," Master's thesis, University of Ottawa, Ottawa, Canada, 2015.

[2] M. S. A. Ahmed, "Run-up distance from deflagration to detonation in fast flames," Master's thesis, Ottawa-Carleton Institute for Mechanical and Aerospace Engineering, University of Ottawa, Ottawa, Canada, 2016.

[3] M. Saif, W. Wang, A. Pekalski, M. Levin, and M. I. Radulescu, *Proc. Combust. Inst.*, 2016, in press.

[4] M. I. Radulescu and B. M. Maxwell, *J. Fluid Mech.*, vol. 667, pp. 96–134, 2011.

[5] Y. J. Zhu, J. Chao, and J. H. S. Lee, *Proc. Combust. Inst.*, vol. 31, pp. 2455–2462, 2007.

[6] G. A. Lyamin, V. V. Mitrofanov, A. V. Pinaev, and V. A. Subbotin, "Propagation of gas explosion in channels with uneven walls and in porous media," in *Dynamic Structure of Detonation in Gaseous and Dispersed Media*, A. Borisov, Ed. kluwer, 1991, vol. 153, pp. 51–75.

[7] A. Teodorczyk, J. H. S. Lee, and K. Knystautas, "Propagation mechanism of quasi-detonations," in *22nd Symp. (Int.) on Combustion*. Pittsburg, PA: The Combustion Inst., 1988.

[8] M. Arienti and J. E. Shepherd, *J. Fluid Mech.*, vol. 529, pp. 117–146, 2005.

[9] C. A. Eckett, J. J. Quirk, and J. E. Shepherd, *J. Fluid Mech.*, vol. 421, pp. 147–183, 2000.

[10] M. I. Radulescu and B. M. Maxwell, *Phys. Fluids*, vol. 22 (6), 2010.

[11] R. I. Soloukhin, *Proc. Combust. Inst.*, vol. 12, p. 799, 1969.

[12] E. A. Lundstrom and A. K. Oppenheim, *Proc. R. Soc. Lond. A*, vol. 310, pp. 463–478, 1969.

[13] M. I. Radulescu, G. J. Sharpe, J. H. S. Lee, C. B. Kiyanda, A. J. Higgins, and R. K. Hanson, *Proc. Combust. Inst.*, vol. 30, pp. 1859–1867, 2005.

[14] A. Makris, A. P. M. Kamel, J. Kilambi, R. Knystautas, and J. H. S. Lee, "Mechanisms of detonation propagation in a porous medium," in *Dynamic Aspects of Detonation*, A. L. Kuhl, J. C. Leyer, A. A. Borisov, and W. A. Sirignano, Eds. American Institute of Aeronautics and Astronautics, 1993, pp. 363–380.

[15] A. Makris, H. Shafique, J. H. S. Lee, and R. Knystautas, *Shock Waves*, vol. 5, pp. 89–95, 1995.

[16] T. Slungaard, T. Engebretsen, and O. K. Sonju, *Shock Waves*, vol. 12, pp. 301–308, 2003.

[17] M. Radulescu, G. Sharpe, and D. Bradley, "A universal parameter quantifying explosion hazards, detonability and hot spot formation: The χ number," in *Proceedings of the Seventh Intational Seminar on Fire and Explosion Hazards*, D. Bradley, G. Makhviladze, V. Molkov, P. Sunderland, and F. Tamanini, Eds. Research Publishing, University of Maryland, 2013, pp. 617–626.

[18] B. M. Maxwell, "Turbulent combustion modelling of fast-flames and detonations using compressible LEM-LES," Ph.D. dissertation, Ottawa-Carleton Institute for Mechanical and Aerospace Engineering, University of Ottawa, Ottawa, Canada, 2016.

[19] S. Menon and A. R. Kerstein, *Turbulent Combustion Modeling: Advances, New Trends and Perspectives*. Springer, 2011, ch. 10: The Linear-Eddy Model, pp. 221–247.

[20] B. M. Maxwell, R. R. Bhattacharjee, S. S. M. Lau-Chapdelaine, S. A. E. G. Falle, G. J. Sharpe, and M. I. Radulescu, *J. Fluid Mech.*, vol. 818, pp. 646–696, 2017.

[21] G. Thomas, R. Bambrey, and C. Brown, *Combust. Theor. Model.*, vol. 5:4, pp. 573–594, 2001.

[22] R. G. Abdel-Gayed, K. J. Al-Khishali, and D. Bradley, *Proc. R. Soc. Lond. A*, vol. 391, pp. 393–414, 1984.